High Performance Thin-Film Transistors with Low-High-Low Band Gap Engineering

Chun-Yen Chang, Yeong-Shyang Lee, Po-Sheng Shih and Chiung-Wei Lin

Department of Electronics Engineering & Institute of Electronics,
National Chiao Tung University, Hsinchu, 300 Taiwan, Republic of China

ABSTRACT

A novel high-performance thin-film transistor (TFT) with low-high-low band gap structure is proposed. We propose a novel device structure combined with low-band-gap materials (microcrystalline Si, μc-Si:H) for the channel region, high-band-gap materials (hydrogenated amorphous silicon, *a*-Si:H) for the source and drain offset regions, and heavily doped low-band-gap materials (n^+ *a*-Si:H) for ohmic contact of source and drain electrodes. We found that, as compared to *a*-Si:H TFT device with conventional inverted-stagger structures, the device with low-band-gap materials in the channel (*e.g.* μc-Si:H) which possesses high conductance can effectively improve the film quality of initial growth active layer near the gate insulator interface and the grown layer. Hence the TFT device parameters such as field effect mobility, threshold voltage, subthreshold swing and ON-current have been significantly improved. This proposed novel structure with high-band-gap material is used to prevent the band to band tunneling and alleviate the high OFF-current in conventional μc-Si:H thin-film transistors. The proposed high performance TFTs with low-high-low band gap structure will have a great impact in application to high resolution thin-film transistor liquid-crystal displays (TFT-LCDs) and active-matrix liquid-crystal displays (AMLCDs).

Keywords: thin-film transistor (TFT), Low-High-Low Band Gap Engineering, hydrogenated amorphous silicon (*a*-Si:H), microcrystalline Si (μc-Si:H) , polycrystalline Si (Poly-Si)

1. INTRODUCTION

The hydrogenated amorphous silicon thin-film transistors (*a*-Si:H TFT's) are used as the dominant pixel switching device in active-matrix liquid-crystal displays (AMLCDs).[1] However, the most serious problems of present *a*-Si:H TFT's development are the low field-effect mobility of carriers and the low reliability in the *a*-Si:H channel, which lead to a low current drivability and device degradation. Hence, many methods for improving the turn-on characteristics of TFT's device have been proposed, including through use of a double gate structure,[2] short channel device[3] or vertical type structure.[4] However, All of these technologies are complicated and difficult to perform. On the other hand, polycrystalline silicon (poly-Si) TFT's improve the current drivability while sacrificing the turn-off capability. For reduction of the higher OFF-state current in poly-Si TFTs, a device using a horizontal offset structure is proposed for reducing the OFF-state current[5]. The conventional horizontal offset structure suppresses the OFF-state carrier conduction effectively due to the carrier

Part of the SPIE Conference on Display Technologies II • Taipei, Taiwan • July 1998
SPIE Vol. 3421 • 0277-786X/98/$10.00

Downloaded From: http://proceedings.spiedigitallibrary.org/ on 04/28/2014 Terms of Use: http://spiedl.org/terms

trapping. However, it needs large device area and other complicated process such as lightly doped implantation, which also needs higher temperature annealing. Meanwhile, new crystalline materials of higher band mobility than that of *a*-Si:H (namely microcrystalline silicon; μc-Si:H) is used to perform high-performance TFTs. It is found that μc-Si:H TFTs also have superior current drivabilities. However, the OFF-state current in their proposed devices are still high and produce a low ON/OFF current ratio of only five orders of magnitude or less.[6-9]

Previously, we have proposed a high-performance TFT with a novel vertical offset structure, whose channel region and offset region are composed of μc-Si:H and *a*-Si:H films, respectively.[10-11] Compared to the conventional inverted-stagger *a*-Si:H TFTs that consisting of a single high-band-gap *a*-Si:H layer, the proposed novel TFT is performed with the insertion of a thin, low-band-gap μc-Si:H layer at the semiconductor/insulator (high-band-gap *a*-Si:H/SiN_x) interface. A high quality, low-band-gap μc-Si:H film is used to enhance the current drivability of this novel device. And, a high-band-gap *a*-Si:H layer is used to suppress the OFF-state leakage current toward a value similar to that of conventional *a*-Si:H TFT's devices. In addition, this novel device use a heavily doped low-band-gap n^+ *a*-Si:H layer as its source/drain ohmic contacts, resulting in a good ohmic contact between semiconductor and metal.

In this paper, we discuss the dependence of device performance on μc-Si:H channel films with various optical band gaps (E_{opt}). Because the fabrication process of the proposed TFTs devices is similar to that used for the conventional inverted-stagger *a*-Si:H TFTs, the area of our device with low-high-low band gap structure can be reduced to smaller than that a conventional horizontal offset device. This will increase the pixel density of TFTs array that would be suitable for applying to future high-definition-television systems (HDTVs). All the films used in our device are deposited of low temperature (≤ 300°C), and the fabrication process is simple and inexpensive with the possibility of high reliability.

2. EXPERIMENTAL

The proposed TFT device with new low-high-low band gap structure is shown schematically in Fig. 1. The fabrication process is similar to the conventional inverted-stagger *a*-Si:H TFT's device except inserting a low-band-gap μc-Si:H film embedded between the gate insulator and undoped *a*-Si:H film. First, a 250nm-thick aluminum film is evaporated on silicon wafers that coated with a 500-nm-thick thermal oxide layer and then patterned to form the gate electrode by photolithography and wet etching. Secondly, a silicon nitride (SiN_x) film as the gate insulator, low-band-gap μc-Si:H and high-band-gap undoped *a*-Si:H compose the compound channel layer. These along with a low-band-gap n^+ *a*-Si:H film are deposited consecutively by a plasma-enhanced chemical vapor deposition (PECVD) system without breaking of the vacuum. The gas mixtures for SiN_x, undoped *a*-Si:H and n^+ *a*-Si:H films are (SiH_4 + NH_3 + N_2), (SiH_4 + H_2) and (SiH_4 + PH_3), and the thickness for SiN_x, undoped *a*-Si:H and n^+ *a*-Si:H films are 300 nm, 140 nm and 70 nm, respectively. The thickness of μc-Si:H films is fixed at 25 nm for these samples with various $[H_2]/\{[SiH_4]+[H_2]\}$ flow rate ratio. The SiN_x film is deposited under conditions of 300°C, 27.78mw/cm^2, and 1 Torr while undoped and n^+ *a*-Si:H films are deposited at 250°C, 25mw/cm^2, 0.3 Torr. In addition, μc-Si:H films are deposited at 250°C, 25mw/cm^2 and 0.55 Torr using a $[H_2]/\{[SiH_4]+[H_2]\}$ flow rate ratio of 980 sccm/(20 sccm + 980 sccm) for 98%-diluted film and 990 sccm/(10 sccm + 990 sccm) for 99%-diluted film, respectively. Thirdly, a 250 nm-thick aluminum film is again evaporated on the grown films and patterned by

Downloaded From: http://proceedings.spiedigitallibrary.org/ on 04/28/2014 Terms of Use: http://spiedl.org/terms

photolithography and wet etching to form source and drain electrodes. Finally, we use CF_4 plasma etching to define the active region of the device and to remove the unwanted n^+ *a*-Si:H layer. The channel width (W) for this device is 120 μm while the channel length (L) is 10μm. All the devices were annealed at 200°C in N_2 ambient for 25 min to form good ohmic contacts. The electrical properties of our novel TFTs were measured by a HP4145B semiconductor parameter measurement system with a PC. The crystallinity of μc-Si:H and *a*-Si:H films is analyzed by Raman scattering spectra. Optical band gap (E_{opt}) is determined from a Tauc plot of the optical absorption coefficient in ~0.4-μm-thick *a*-Si:H and μc-Si:H films, which are deposited under identical conditions, except the flow rate of hydrogen and silane gas.

3. RESULTS AND DISCUSSION

In this paper, we discuss the performance of TFT devices with the low-high-low band gap structure compared with that of control devices without inserting a μc-Si:H channel layer. The E_{opt} of *a*-Si:H films prepared with various conditions of deposition is different. The E_{opt} of undoped *a*-Si:H film used as the channel layer of control devices is ~1.68 eV, which is higher than that of 98%-diluted μc-Si:H films (E_{opt} ~ 1.43 eV) and 99%-diluted μc-Si:H films (E_{opt} ~ 1.59 eV). In addition, the E_{opt} of n^+ *a*-Si:H films used for all devices is ~1.48 eV.

Figures 2 and 3 show the transfer curves for devices with μc-Si:H channel layer of various E_{opt} values, at V_{ds}=15V and V_{ds}=1V, respectively. All the devices have good performances including small threshold voltages and sharp transition regions. As shown in Fig. 2 and Fig. 3, the presence of a low-band-gap μc-Si:H channel layer improves the ON-state characteristics, and the high-band-gap *a*-Si:H offset layer suppresses the OFF-state leakage current due to the band-to-band tunneling (BBT). For convenience of comparison, we denote the devices of 98%-diluted (E_{opt} ~ 1.43 eV) and 99%-diluted (E_{opt} ~ 1.59 eV) μc-Si:H channel as A and B, respectively. Although the ON-state current of device A is higher than that of device B, the OFF-state current of device A is still lower than that of device B, as shown in Fig. 2 and Fig. 3. We believe that this is dominantly due to the discontinuity of valence band between low-band-gap channel layer and high-band-gap offset layer. The more higher difference in the valence band discontinuity between low-band-gap channel layer and high-band-gap offset layer, the more effective hole confinement on suppressing the OFF-state leakage current.[12] The band discontinuities between low-band-gap channel layer (μc-Si:H) and high-band-gap offset layer (*a*-Si:H) for devices A and B are ~0.25 eV and ~0.09 eV, respectively. Therefore, the effect of suppressing the OFF-state leakage current at device A is noticeable than that at device B. The devices with low-high-low band gap structure reveal higher current driving capabilities than the control device (conventional *a*-Si:H TFT's). The transconductance g_m, which is defined by $\delta I_{ds}/\delta V_{gs}\,|_{V_{ds}\text{ is fixed}}$, is an important parameter that related to the frequency response. The g_m is proportional to the operating frequency.[13] Fig. 4 demonstrates the dependence of transconductance on gate voltage. The highest transconductance occurs on device A with 98%-diluted μc-Si:H channel, which means that it works very fast. The excess H_2 plasma enhances the formation of new defect, hence the device B with 99%-diluted μc-Si:H channel exhibits a smaller transconductance value than that of device A. However, all the devices with low-band-gap μc-Si:H channel work faster than the control device.

From Fig. 2 and Fig. 3, the current density of ON-state is increased from 6.55 mA/m (control device) to 8.26 mA/m (device A with 98%-diluted μc-Si:H channel), then decays to 7.44 mA/m (device B with 99%-diluted μc-Si:H channel). The devices

Downloaded From: http://proceedings.spiedigitallibrary.org/ on 04/28/2014 Terms of Use: http://spiedl.org/terms

with low-band-gap μc-Si:H channel can not only improve the OFF-state characteristics but also possess higher driving currents indeed. The higher ON-current density is due to less bulk trap density. We have measured and deduced the density of deep gap states (N_{deep}) according the equation: $N_{deep} = C_{ins}S(qkt)^{-1}$. The density of deep gap states (N_{deep}) of these devices decreases from 7.34 x 10^{12} $cm^{-2}eV^{-1}$ (control device) to 6.28 x 10^{12} $cm^{-2}eV^{-1}$ (device B with 99%-diluted μc-Si:H channel) then decreases to 4.79 x 10^{12} $cm^{-2}eV^{-1}$ (device A with 98%-diluted μc-Si:H channel), where S is the subthreshold swing. The density of deep gap states (N_{deep}) is dependent on the quality of a-Si:H or μc-Si:H films, and the optical band gap (E_{opt}) is also dependent on the quality of a-Si:H or μc-Si:H films. Figure 5 demonstrates the dependence of the N_{deep} on the optical band gap (E_{opt}) of channel in devices.

Figure 6(a) demonstrates the variation of subthreshold swing (S) with optical band gap (E_{opt}) of channel in devices, which behaves as a trend similar to the density of deep gap states (N_{deep}). The subthreshold swing decreases from 1.01 V/dec (control device with a-Si:H channel whose E_{opt} ~1.68 eV) to 0.96 v/dec (device B with 99%-diluted μc-Si:H channel whose E_{opt} ~ 1.59 eV) then decreases to 0.68 V/dec (device A with 98%-diluted μc-Si:H channel whose E_{opt} ~ 1.43 eV). In addition, smaller threshold voltages (V_t) are obtained for our novel devices as shown in Fig. 6(b), in which 1.08 V, 1.65 V and 1.91 V are obtained for A, B and control device, respectively.

Figure 7(a) demonstrates that the performance of devices with low-high-low band gap structure does not degrade by inserting a high quality, low-band-gap μc-Si:H film. The ON/OFF current ratio increases from 6.19 x 10^5 (control device with a-Si:H channel whose E_{opt} ~1.68 eV) to 8.30 x 10^5 (device B with 99%-diluted μc-Si:H channel whose E_{opt} ~ 1.59 eV) then increases to 7.30 x 10^6 (device A with 98%-diluted μc-Si:H channel whose E_{opt} ~ 1.43 eV). Here the ON/OFF current ratio is defined as the ratio of I_{ds} (ON)$|_{Vgs=20V,Vds=1V}$ to I_{ds} (OFF)$|_{Vgs=-1V,Vds=1V}$. Finally, the dependence of the field effect mobility (μ_{FE}) on optical band gap (E_{opt}) of channel layer is shown in Fig. 7(b). The H_2 gas dilution method produces high quality μc-Si:H film with less defect centers and lower optical band gap (E_{opt}). Hence the density of scattering center which limit the field mobility is reduced. The speeds of devices with low-band-gap μc-Si:H channel are enhanced with higher field effect mobility than the control device of 1.02 cm^2/V-s. Device A (with 98%-diluted μc-Si:H channel whose E_{opt} ~ 1.43 eV) has a much higher field effect mobility of 2.88 cm^2/V-s while 1.64 cm^2/V-s for device B (with 99%-diluted μc-Si:H channel whose E_{opt} ~ 1.59 eV) due to the H_2 plasma etching induced damage during the deposition. These field effect mobility are measured in the saturated region and deduced from the equation: $I_{ds} = \mu_{FE}C_{ins}W(V_{gs}-V_{th})^2/2L$. Here μ_{FE}, C_{ins} is the field effect mobility and gate insulator capacitor respectively.

4. CONCLUSION

A novel high-performance thin-film transistor (TFT) with low-high-low band gap structure, which can be performed easily under conventional TFT fabrication process, has been proposed and fabricated. A high-band-gap material is embedded vertically between channel and source/drain contacts in this proposed structure. The high-band-gap offset layer, which blocks the carrier conduction at OFF-state of device, is used to prevent the band to band tunneling and alleviate the high OFF-current in conventional thin-film transistors. This proposed structure used low-band-gap material as its channel can improve the device performance, such as current driving capability (ON-state current), field-effect mobility, and so on,

Downloaded From: http://proceedings.spiedigitallibrary.org/ on 04/28/2014 Terms of Use: http://spiedl.org/terms

while the high-band-gap material is used to suppress the leakage current due to band to band tunneling (BBT), i.e. gate-induced drain leakage current (GIDL). In addition, this structure used heavily doped low-band-gap material as its source/drain ohmic contacts can obtain the good ohmic contacts between semiconductor and metal. Furthermore, various materials (for example, VI-VI, III-V, II-VI alloys, and so on) can be widely applied to fabricate the low-band-gap channel, high-band-gap offset layer, and low-band-gap ohmic contacts for this proposed TFT device with low-high-low band gap structure.

5. ACKNOWLEDGEMENTS

The authors would like to express their appreciation to the staff of the Semiconductor Research Center, National Chiao Tung University for their technical support. This work was supported by the National Science Council of the Republic of China under contract No. NSC87-2215-E009-061.

6. REFERENCES

1. N. Ibaraki, "Technical issues for 40-inch a-Si:H TFT," *AM-LCD'95 Dig.*, Japan, pp. 67-70, 1995.
2. Y. Kaneko, K. Tsutsui, H. Matsumaru, H. Yamamoto and T. Tsukada, "Amorphous silicon thin film transistor with a buried double-gate structure," *IEDM Tech. Dig.*, pp. 337-340, 1989.
3. Y. Uchida and M. Matsumura, "Short channel a-Si:H thin-film MOS transistor," *IEEE Trans. Electron Devices*, vol. ED-36, pp. 2940-2943, 1984.
4. Y. Uchida and Y. Nara and M. Matsumura, "Proposed vertical-type amorphous-silicon field-effect transistor," *IEEE Electron Device Lett.*, vol.EDL-5, pp. 105-107, 1984.
5. T. Y. Huang, I. W. Wu, A. G. Lewis, A. Chiang and R. H. Bruce, "A simple 100-V polysilicon TFT with improved turn-on characteristics", *IEEE Electron Device Lett.*, vol. EDL-11, pp. 244-246, 1990.
6. S. S. He and G. Lucovsky, "A low temperature plasma-assisted deposition process for microcrystalline thin film transistor, TFTs," *Mat. Res. Symp. Proc.*, vol. 336, pp. 25-30, 1994.
7. K. C. Hsu, B. Y. Chen, H. T. Hsu, K. C. Wang, T. R. Yew and H. L. Hwang, "Thin film transistor made from hydrogenated microcrystalline silicon," *Japan J. Appl. Phys.*, vol. 33, pp. 639-642, 1994.
8. C. W. Liang, W. C. Chiang and M. S. Feng, " Microcrystallinity of undoped amorphous silicon film and its effects on the transfer characteristics of thin-film transistor," *Japan J. Appl. Phys.*, vol. 34, pp. 5943-5948, 1995.
9. C. C. Tsai, G. B. Anderson and R. Thompson, "Growth of amorphous, microcrystalline, and epitaxial silicon in low temperature plasma deposition," *Mat. Res. Proc.*, vol. 192, pp. 475-480, 1990.
10. C. Y. Chang and C. W. Lin, "A High-Performance Thin-Film Transistor with a Vertical Offset Structure," *IEEE Electron Device Lett.*, vol. EDL-17, pp. 572-574, 1996.
11. C. Y. Chang and C. W. Lin, "A Novel Thin-Film Transistor with Vertical Offset Structure," *Japan J. Appl. Phys.*, vol. 36, pp. 2032-2043, 1997.
12. P. M. Garone, V. Venkataraman, and J. C. Sturm, "Hole Confinement MOS-gated GexSi1-x/Si Heterostructures," *IEEE Electron Device Lett.*, vol. EDL-12, pp. 230-232, 1991.
13. S. M. Sze, *Physics of Semiconductor Devices*, pp. 440-447, Wiley, New York, 1981 (2nd ed.).

Downloaded From: http://proceedings.spiedigitallibrary.org/ on 04/28/2014 Terms of Use: http://spiedl.org/terms

Fig. 1: A schematic diagram of the proposed novel thin-film transistor device with low-high-low band gap structure.

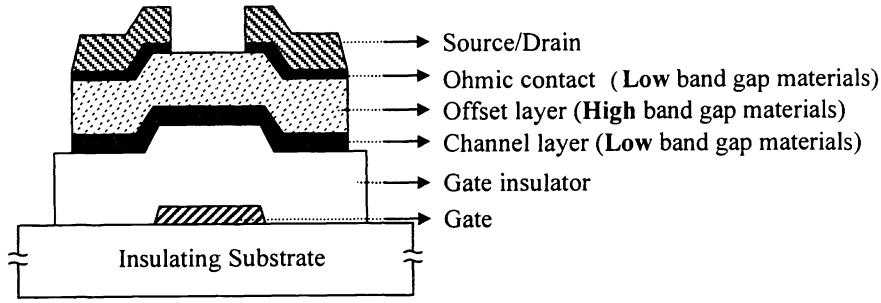

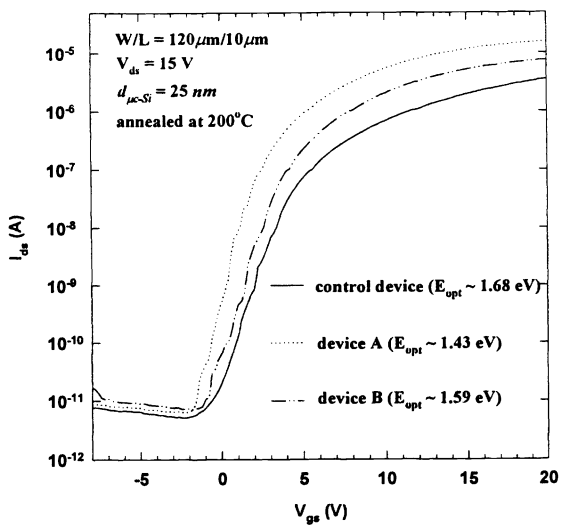

Fig. 2. The dependence of transfer at large V_{ds} (=15V) on devices with various channel layers.

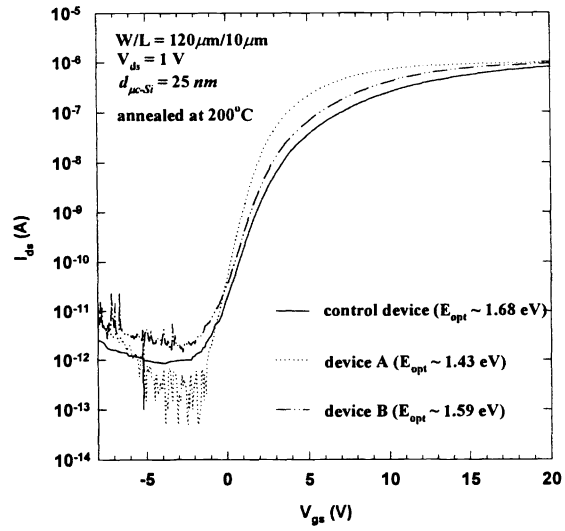

Fig. 3. The dependence of transfer at small V_{ds} (=1V) on devices with various channel layers.

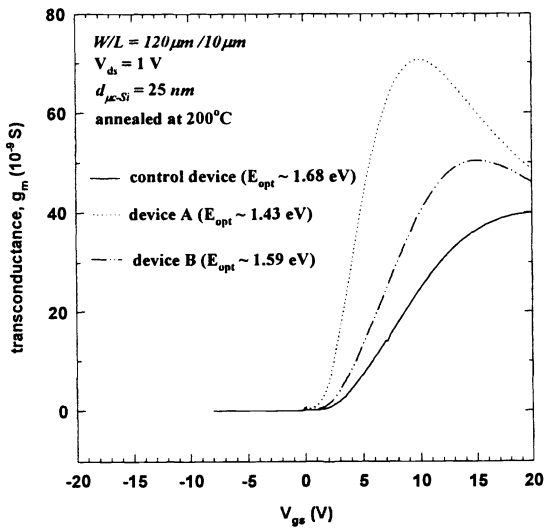

Fig. 4. The dependence of transconductance characteristics on devices with various channel layers.

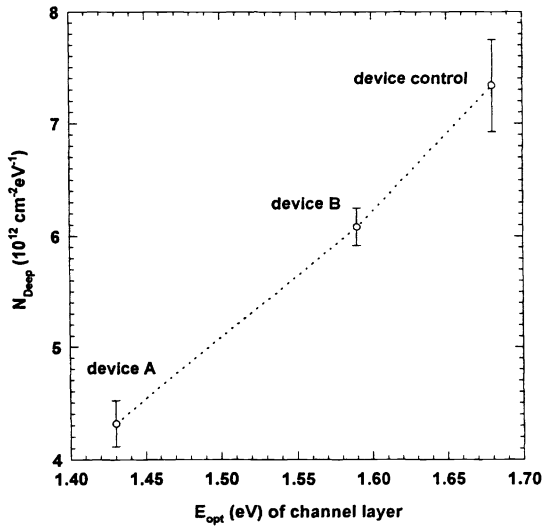

Fig. 5. The dependence of deep gap state density on devices with various E_{opt} values of channel layer.

Downloaded From: http://proceedings.spiedigitallibrary.org/ on 04/28/2014 Terms of Use: http://spiedl.org/terms

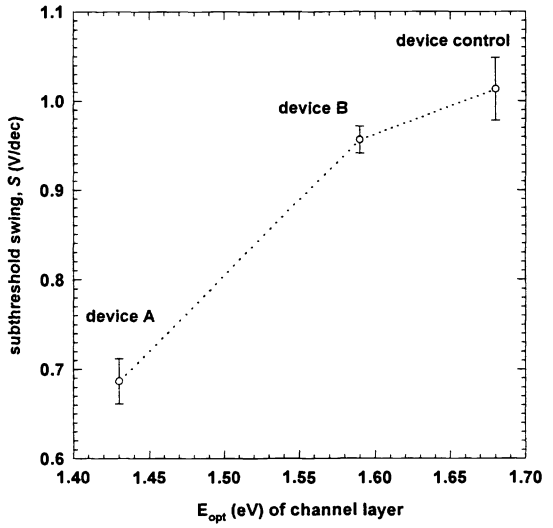

Fig. 6(a). The dependence of subthreshold swing on devices with various E_{opt} values of channel layer.

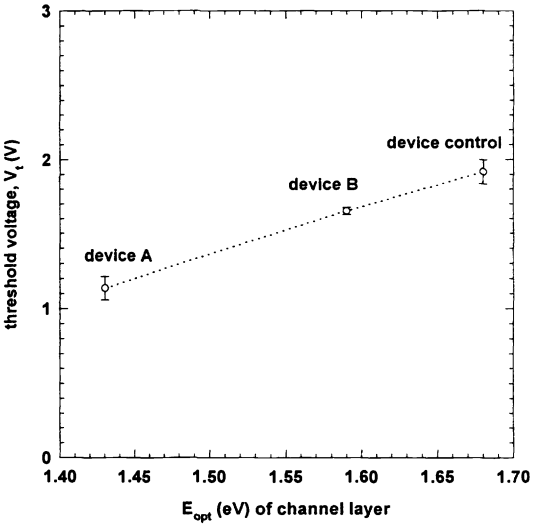

Fig. 6(b). The dependence of threshold voltage on devices with various E_{opt} values of channel layer.

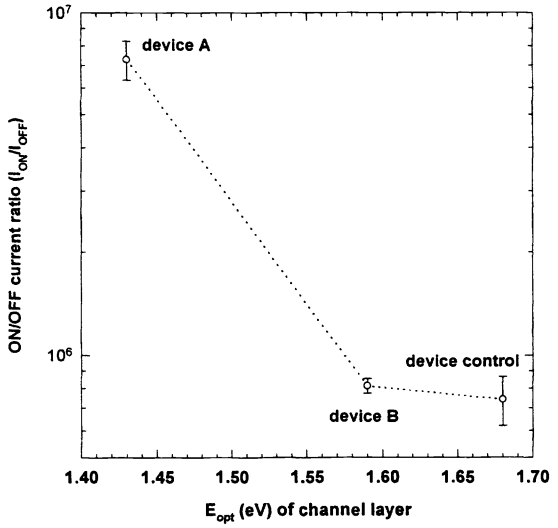

Fig. 7(a). The dependence of ON/OFF current ratio on devices with various E_{opt} values of channel layer.

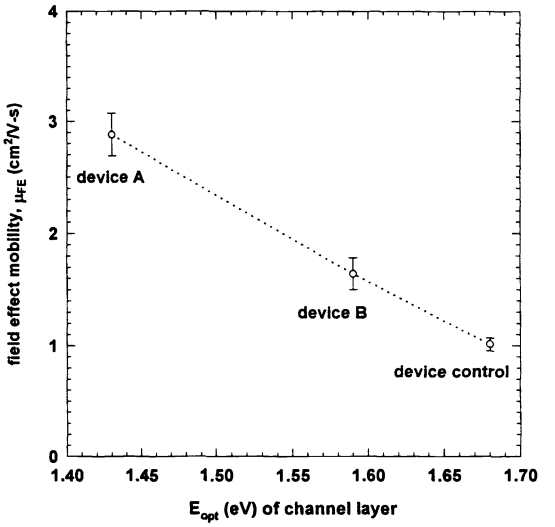

Fig. 7(b). The dependence of effect field mobility on devices with various E_{opt} values of channel layer.

Downloaded From: http://proceedings.spiedigitallibrary.org/ on 04/28/2014 Terms of Use: http://spiedl.org/terms